THE WORLD OF INNOVATIONS

https://doi.org/10.15407/scine16.05.090

CHEBERIACHKO, S.I., CHEBERIACHKO, Yu.I., and SHAIKHLISLAMOVA, I.A.
Dnipro Polytechnic National Technical University,
19, D. Yavornytskyi Ave., Dnipro, 49005, Ukraine,
+380 56 744 1411, +380 56 247 0810, rector@nmu.org.ua

DESIGNING OF HALF-MASKS FOR FILTERING RESPIRATORS

Introduction. *Diseases of the respiratory system head the list of occupational diseases. They are caused by pollution of the working zone air with harmful aerodispersed particles, use of improper individual respiratory protective devices.*

Problem Statement. *The efficiency of filtering respirators depends on two components: time of protective effect and insulating properties of half-masks. This requires conducting relevant research in order to design the half-masks which allow providing high insulating properties.*

Purpose. *Improvement of protective effect of filtering respirators by improving their design with respect to anthropometric peculiarities of workers' faces.*

Materials and Methods. *To develop the surface of a half-mask, the equation of free energy of a bent optional plate was used, which is outlined with a two-dimensional spline-surface, its unknown coefficients are defined by the method of proportional parts based on the data of three dimensional coordinates of the key points of anthropometric facial features.*

Results. *Regularities of forming the surface of half-masks were defined based on the data of three dimensional coordinates of the key points of anthropometric facial features. A method was developed for measuring the temperature of obturator surface with a thermal imagery device based on output signal processing, which allows carrying out on-line control of areas where gaps occur along the obturation line as well as defining deterioration of insulating properties of a dust mask and estimating its protection factor.*

Conclusion. *The algorithm of half-mask design was developed with respect to the results of 3D scanning of faces, digital models of head developing as well as half-masks surface and obturator construction associated with them. The reasonable parameters of filtering box, size of ioutlet for providing the minimum pressure difference and regular dust distribution on filtering surface were determined.*

Keywords: model, half mask, respirator, obturator, insulation coefficient.

In 2017—2018, among occupational diseases the most widespread were respiratory diseases, as their share accounted for 40.1% of the total number of occupational diseases resulting from work in areas contaminated with harmful airborne particles (dust, smoke, fog), gases, and vapors, as well as the lack personal protective equipment for respiratory organs (PPERO) or use of those that do not meet the requirements for their functional

Citation: Cheberiachko, S.I., Cheberiachko, Yu.I., and Shaikhlislamova, I.A. Designing of Half-Masks for Filtering Respirators. *Sci. innov.* 2020. V. 16, no. 5. P. 90—102. https://doi.org/10.15407/scine16.05.090

purpose and anthropometric dimensions of the user faces.

Elastomeric half masks are an integral part of reusable filter respirators. Reliable fit to the face, level of comfort, possibility of communication depends on their design [1]. Numerous studies to determine the effectiveness of respirators in real operating conditions have shown that with the right choice of filter, the overall effectiveness of PPERO is determined by the infiltration of unfiltered air through the gaps between the front half mask (respirator) and face. This path is the main route of penetration of polluted air into the respiratory system. The occurrence of gaps depends on many factors: the face anthropometry, design of the headgear and obturator, and others. In this case, their size is a variable. As a result, the protection factor (PF) may vary dozens of times in several minutes [2]. Therefore, the author's research aims at establishing the basic laws of formation of structures of elastomeric half masks in order to raise their effectiveness.

Reliable insulation of the respiratory organs by half masks is inextricably linked with face anthropometric points. One of the most problematic places where most often there are gaps in the obturation strip is the area of the bridge of the nose [3], as about 84% of the gaps is reported in there (near the nose and cheeks). Also, when checking the insulating properties of PPERO negative results are reported during conversation (facial expressions). Most experts see the solution to this problem in a detailed study of the anthropometric characteristics of the face in order either to identify the most influential dimensions on the insulating properties or to calculate universal "components" that take into account all the measured parameters of the face.

Thus, the task is to study the influence of face anthropometric characteristics on the design of the frame of elastomeric half masks, which would provide its high insulating properties.

The manufacture of half masks is a complex process consisting of the development of design documentation, terms of reference, predesign and detailed design, and specifications [4]. The implementation of these stages requires a significant amount of time and appropriate professional skills. The present-day development of industry constantly requires reducing the time for these processes while keeping the quality of final product. Various approaches have been proposed for this, in particular the use of automated design systems. However, designing respirators has not been sufficiently formalized and, as a rule, uses heuristic methods that are based mainly on the designer's erudition and intuition [5—7]. This contributes to errors and the loss of time to correct them. According to the experts, the biggest problem is the lack of systematic data on the influence of technological processes on the general quantitative or qualitative patterns of phenomena occurring in protective equipment [8]. It is believed that their design takes the most time while designing half

Table 1. **Correlation between the Face Parameters and the Insulating Properties of Half Masks**

Respirator model	Number of persons involved in study	Critical anthropometric points	Source
Half mask U.S. Safety Series 200	39 men, 34 women	Nose length, face length and lip length	[17]
Half mask U.S. Safety Series 200	38 men, 30 women	Nose length, face length and lip length	[18]
AO 5-Star Series, North 770 Series, Survivair Series 2000	20 men, 21 women	Face length, face width	[19]
Half mask MSA Advantage	186 persons	Length and protrusion of the nose	[20]
Half mask Youngsung Co. YS1050DS Samgong Co. SG5121 3M Co. Series 6000	150 Korean persons: 112 men, 38 women	Face width and protrusion of the nose	[21]
18 models of filtering half masks N95 certified by NIOSH	15 men, 18 women	Face width, protrusion of the nose, and face length	[22]

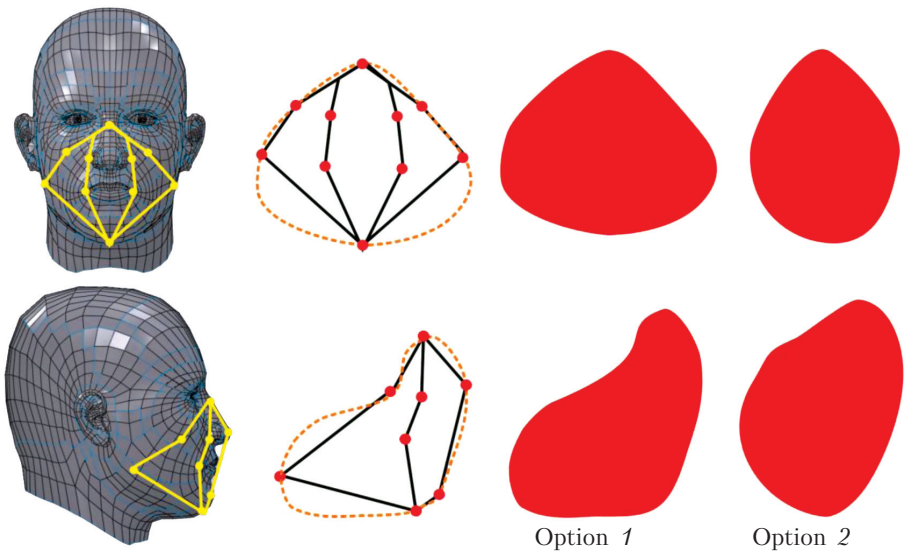

Fig. 1. Schematic representation of the projection of the contours of the obturation strip of half masks [23]

masks [9], as the main problems are related to providing adequate protection to as many people with different anthropometric facial features, as possible. given variability of working conditions and their significant impact on human physical and mental conditions. There are many publications where the effect of one or another factor on the quality of the respirator has been studied in detail [10–16]. For example, a database of anthropometric data has been compiled [16]; the influence of a respirator on the physiological state of workers has been studied [12]; changes in the protection effectiveness, depending on operating conditions, has been evaluated [13. 14], etc. This has enabled designing respirators from different blocks, but there is a need to generalize the known data and, accordingly, to combine them into a specific algorithm for designing respirators.

The purpose of this research is to develop an algorithm for designing an elastomeric half mask with high insulating properties.

To solve the outlined task, it is necessary to identify critical points on the worker face; to develop a 3D model of the human head and, accordingly, a 3D model of elastomeric half masks; to calculate the area of the obturator fit to the face and insulation coefficient of the designed half masks. To solve the problem of determining the critical points on the human face to build a correct model of a half mask we have used publications of famous American researchers [17—22], which include the most important parameters: face length and width, nose length, lip length, nose height, etc. (Table 1).

According to the recommendations, these anthropometric parameters of the face can be measured using a caliper and measuring tape or by 3D-scanning (Fig. 1). Earlier, the authors conducted relevant studies [16] in which they measured the facial dimensions of more than 400 people of different sexes (employees and students of the Mining University (Dnipro)) (Table 2). Their face length ranges within 98.5—143.2 mm, and width varies within 131.3—164.9 mm. The generalized results are given in Table 3.

There are two approaches to determining the key points at which one can get the contour of elastomeric half mask. The first one is based on data from the parametric table of the U.S. National Institute for Occupational Safety and Health (NIOSH). It is assumed that the most important for the design of half masks are the size of the face

height and the lip length. The second approach proposed by Z. Zhuang is based on complex parameters, the so-called components PC1 and PC2, which include almost all the studied parameters.

The following components are calculated by the formulas [22]:

$$\mathbf{PC1} = 0.343264 \times \text{GONI} + 0.372717 \times \text{ZYGO} + \\ + 0.329648 \times \text{MENSELL} + 0.363474 \times \text{MSNL} + \\ + 0.113578 \times \text{NOSEPRH} + 0.301125 \times \\ \times \text{NOSEBRTH} + 0.202311 \times \text{LIPLGTHH} + \\ + 0.193650 \times \text{NOSEPRH}.$$

$$\mathbf{PC2} = -0.152951 \times \text{GONI} - 0.039087 \times \\ \times \text{ZYGO} - 0.093279 \times \text{MENSELL} + 0.359799 \times \\ \times \text{NOSEPRH} - 0.173099 \times \text{LIPLGTHH} + \\ + 0.013306 \times \text{LIPLGTHH} + 0.551842 \times \\ \times \text{LIPLGTHH} - 0.210833 \text{ MSNL}.$$

Table 2. **Anthropometric Data of the Human Face**

Critical point	Abbreviation	Parameter
Face width at the eye line	GONI	Maximum horizontal width of the face between the extreme points of the eye sockets
Face width at the line of the lower jaw corners	ZYGO	Maximum horizontal width of the face between the jaw arches
Nose width	NOSEBRTH	Distance between the right and the left points of the nose wings
Lip length	LIPLGTHH	Distance between the right and the left points at the mouth corners
Face length	MENSELL	Distance between the lower point of the chin and the upper point of the nose cavity
Nose length	NOSEPRH	Distance between the lower point of the nose and the upper point of the nose cavity
Face lower part	MSNL	Distance between the lower point of the chin and the lower point of the nose

Table 3. **Generalized Anthropometric Parameters of the Human Face. mm [16]**

Parameter	Men (320 persons)	Women (80 persons)	Average
GONI	144.3 ± 8.9	135.3 ± 6.0	144.5 ± 8.9
ZYGO	130.2 ± 9.1	121.1 ± 9.1	128.4 ± 10.1
NOSEBRTH	32.7 ± 1.9	29.6 ± 3.3	32.0 ± 3.6
LIPLGTHH	51.4 ± 3.7	45.0 ± 3.7	48.7 ± 4.8
MENSELLH	121.1 ± 8.4	115.2 ± 5.8	119.8 ± 7.8
NOSEPRH	24.1 ± 2.7	22.4 ± 2.2	23.9 ± 2.6
MSNL	49.3 ± 4.5	43.2 ± 3.0	47.7 ± 5.0

Fig. 1 schematically shows the critical points for obtaining the geometry of half mask for the two options. The first option, in addition to the face length and lip length, also takes into account the face width and the nose width. The second option also takes into consideration the face width at the level of the lower jaw.

Development of Face 3*D*-Model

The face 3D model shall contain a polygonal grid, the apexes of which converge at key anthropometric points that define the contours of the face.

To do this, the coordinates of anthropometric points on the scanned images of faces have been determined, using a software with 3D-reconstruction function:

$$\begin{pmatrix} x \\ y \\ z \end{pmatrix} = reconstruct\,(u, v, i, k, P_c, P_p)$$

where P_c, P_p are projection matrixes of the camera and projector, which are determined in the calibration process; u, v are coordinates of points determined by digital image analysis and backlight pattern identification algorithms, which are by a matrix of color pixels I, enable obtaining an infinite number $\left\{\mu_k = < \begin{pmatrix} u_k \\ v_k \end{pmatrix}, i_k > \right\}$ of identified pattern points; i is index of straight line of pattern; k is adjustment factor of scanned image data matrixes.

In the future, as a result of multi-stage assessment of the proportions of the head represented by a cloud of points (Fig. 2. a). using the weighted Gaussian function. radial view and local fit, given the topological structure a digital image has been formed. So, at the first stage, the coordinates $d = (d_1, d_1, ..., d_N)$, that represent a set of vectors $d_i = (d_1^i, d_2^i, ..., d_N^i)$, the elements of

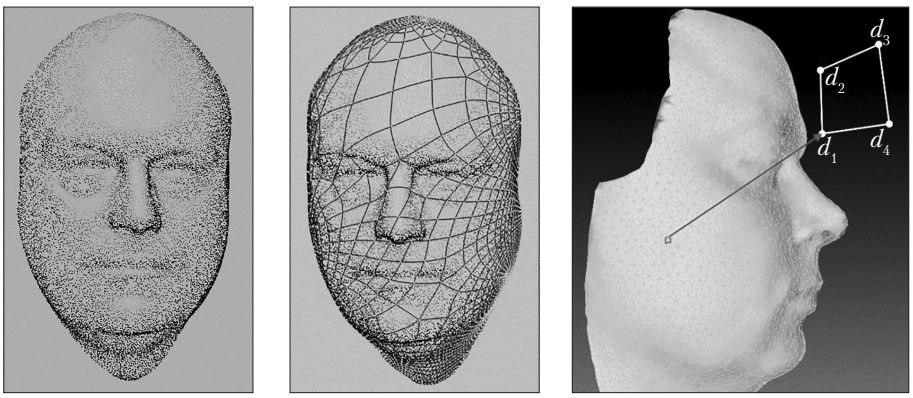

a *b* *c*

Fig. 2. Stages of conversion of the scanned image of the head from a cloud of points (*a*) with the applied splines (*b*) in digital form with layout and coordinates (*c*)

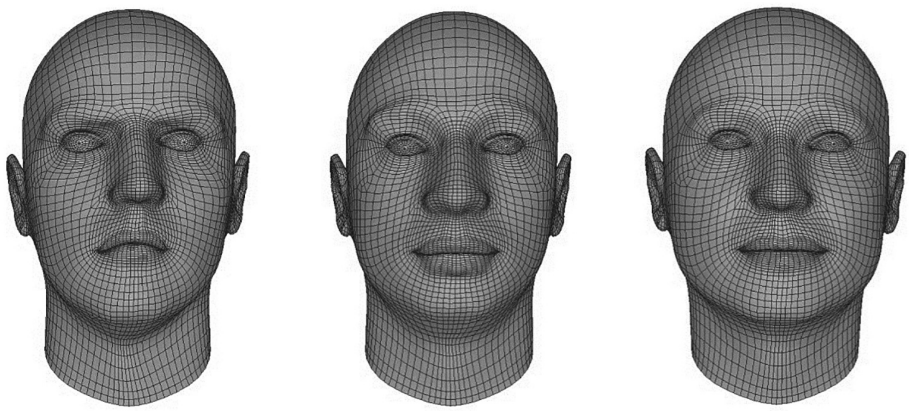

a *b* *c*

Fig. 3. Digital models of the head with different anthropometric parameters: *a* — the first size; *b* — the second standard size; *c* — the third standard size

which are model apex indexes are given. The vector defines a broken line that describes one characteristic feature of the face, the contour of the nose, the lips or the face as a whole. The line dimensions are set using anthropometric points defined on the face. The lines form a parabolic spline that continuously sets the shape of the intersection (Fig. 2, *b*). Each spline is evenly divided by additional points to form an equal number of sections on all horizontal intersections. Additional points are combined with each other, forming a grid of quadrangles (Fig. 2, *c*). When fitting the layout to the anthropometric points, the three types of transformations are used: identical, displacement relative to the established points, and affine transformation relative to the already placed points.

For the "exact" stages of fit of individual features, the Nelder–Mead method is used. It allows working with a wide class of deformable models and making corrections at any stage in the case of incorrect data input, heavily “contaminated” images, and other defects (Fig. 3).

The difference between this model and the known ones is the absence of an intermediate stage that is adjusted to the anthropometric points on the scanned image, and a polygonal model is built on its basis. Hence, the offered model provides for, at first, a rough adjustment by means of interactive algorithm and later on, an exact fit by splines.

3*D*-Model Half Mask

3*D*-modeling of half mask has been made using a special function determined by the method of linear interpolation. It allows setting the shape of the curve at the control points that, in our case, correspond to the key anthropometric dimensions. The coordinates of the points are given from the parametric model of the head.

Let function $f(x)$ is known only in the nodes of a certain grid set by the table $\{x_i, f_i = f(x_i), i = \overline{1, N}\}$. For determining this unknown function, let use firstly build other function $\varphi(x; a)$, that depends on the vector of parameters $a = (x_i, a_1, ..., a_N)^T$, in such a way as

$$\varphi(x_i; a_1 \ldots\ldots a_N) = f_i, \quad i = \overline{1, N}.$$

For solving this problem, let us consider a linear interpolation. In this case, the given function can be written as

$$\varphi(x; a_1 \ldots\ldots a_N) = \sum_{k=1}^{N} a_k \varphi_k(x),$$

where $\varphi_k(x)$, $k = 1$, N is a set of certain given functions.

In order to find the parameters a, it is necessary to solve the system of linear equations:

$$\sum_{k=1}^{N} a_k \varphi_k(x_i) = f_i.$$

Let us use a known approach to determine the spline function that meets the conditions of interpolation in the nodes of function $\varphi(x; y)$ fused by the condition of continuity. Consider the equation of total free energy of a curved plate that is described by a 2D spline surface [25]:

$$\varphi(x, y) = \sum_{i=1}^{N} C_i \left[(x - x_i)^2 + (y - y_i)^2\right] \times$$
$$\times ln\left[(x - x_i)^2 + (y - y_i)^2\right] + Ax, By + D.$$

Coefficients C_1, C_2, ...C_i, A, B, D are determined from the equations $\varphi(x_i, y_i) = f_i$, $i = \overline{1, N}$; $\sum_{i=1}^{N} C_i = 0$; $\sum_{i=1}^{N} C_i x_i = 0$; $\sum_{i=1}^{N} C_i y_i = 0$. To calculate coefficients, the two matrixes based on the nine available coordinates have been composed (Fig. 4):

$$z_1(x_1, y_1) = C_1\left[(x - x_1)^2 + (y - y_1)^2\right] \times$$
$$\times ln\left[(x - x_1)^2 + (y - y_1)^2\right] + Ax_1, By_1 + D;$$
$$z_2(x_2, y_2) = C_1\left[(x_1 - x_2)^2 + (y_1 - y_2)^2\right] \times$$
$$\times ln\left[(x_1 - x_2)^2 + (y_1 - y_2)^2\right] + Ax_2, By_2 + D;$$
$$z_N(x_N, y_N) = C_N\left[(x_{N-1} - x_N)^2 + (y_{N-1} - y_N)^2\right] \times$$
$$\times ln\left[(x_{N-1} - x_N)^2 + (y_{N-1} - y_N)^2\right] +$$
$$+ C_N\left[(x_{N-1} - x_N)^2 + (y_{N-1} - y_N)^2\right] + Ax_2, By_2 + D;$$
$$0 = C_1 + C_2 + C_3 + ... + C_N;$$
$$0 = C_1 x_1 + C_2 x_2 + C_3 + ... + C_N x_N;$$
$$0 = C_1 y_1 + C_2 y_2 + C_3 + ... + C_N y_N.$$

As a result of calculations, the coefficients for the function that describes the spline surface interpolating the values of the specified points have been obtained, where $A = -0.56$; $B = 0.87$; $D = 16.3$:

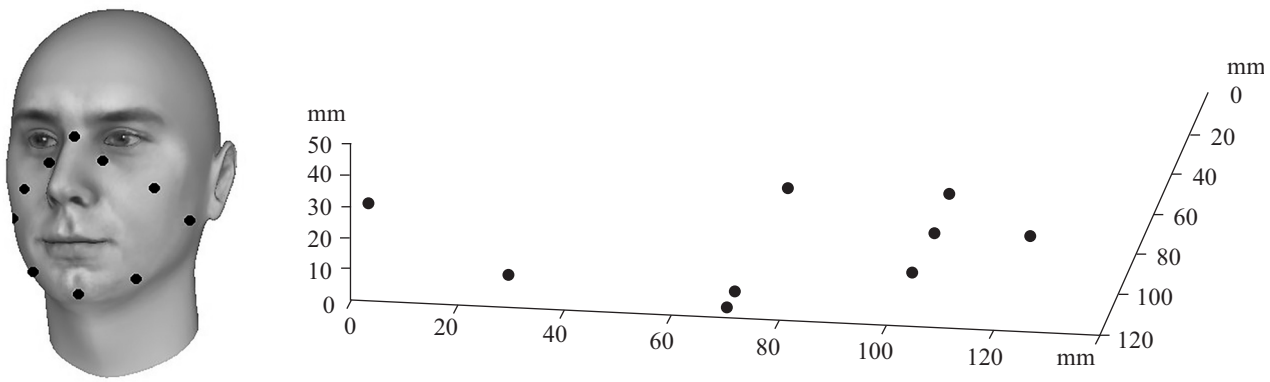

Fig. 4. Key anthropometric points of the face. transferred to a 3D coordinate system: *a* — the position of key points on the 3D image of the face; *b* — the position of key points on the grid

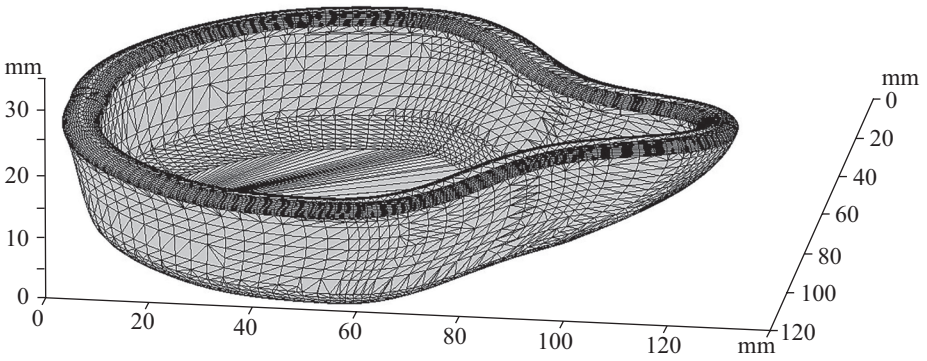

Fig. 5. The half mask surface obtained by linear interpolation

$$X:=\begin{pmatrix}65.5\\105.6\\130.3\\62.5\\0\\35.6\\65.2\\65.2\\65.2\end{pmatrix}\quad Y:=\begin{pmatrix}120.5\\100.3\\70.6\\0\\70.6\\100.3\\35.3\\70.6\\100.3\end{pmatrix}\quad Z:=\begin{pmatrix}30.5\\30.5\\40.0\\30.5\\30.5\\30.5\\15.2\\0\\10.2\end{pmatrix}\quad C:=\begin{pmatrix}2.479\\3.113\\10.177\\-0.393\\2.236\\-0.18\\0.56\\5.4\\-2.1\end{pmatrix}.$$

Based on the expression of the obtained function, the surface of the half mask has been built (Fig. 5). It passes through certain points and uses them as interpolation nodes.

Based on the obtained surface, two types of elastomeric half-mask design have been created (Fig. 6). The first option takes into consideration the face width and the nose width, the distance from the nose to the chin and the face width at the level of the lower jaw corners. In the second option, the distance from the nose to the chin, the nose width, and the lip length are taken into account. Based on the obtained data and average measurements given in Table 3, it has been proposed to place key points for constructing an obturation strip on the face. The nose width and the distance from the nose to the chin are the same in both cases. The difference is the possibility of choosing either the face width or the lip length. Thus, the obturator contour is narrow at the top of the face and widens to the bottom to cover the

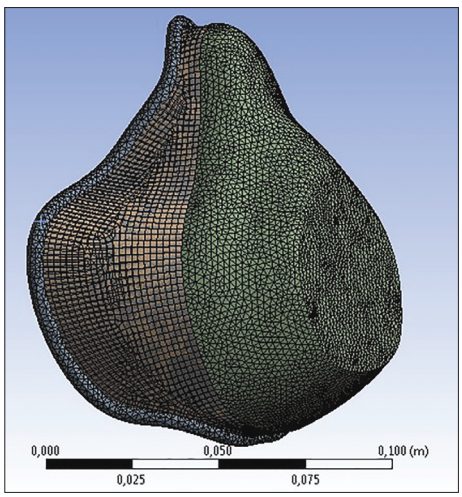

a

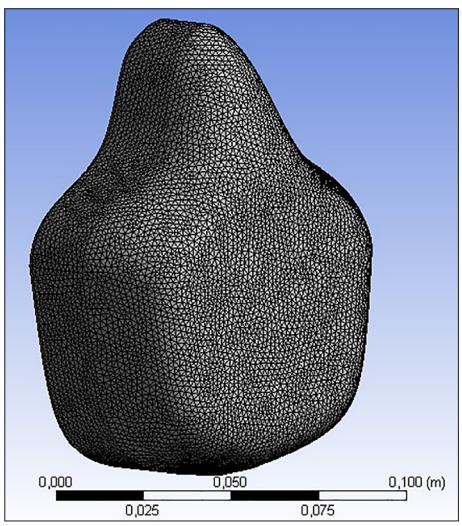

b

Fig. 6. 3*D*-models of elastomeric half masks made according to the design of option 1 (*a*) and option 2 (*b*)

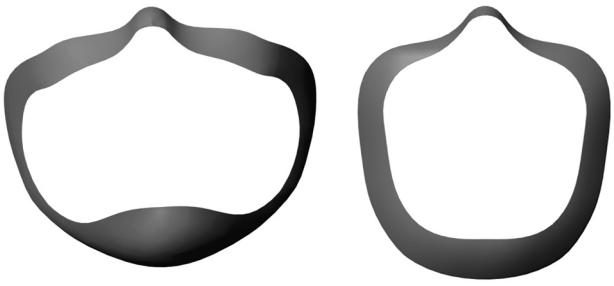

a *b*

Fig. 7. The area of contact of the half mask with the face (obturation strip) in the model according to option 1 (*a*) and in the model according to option 2 (*b*)

cheeks. In our opinion, in the first case, the influence of facial expressions during conversation and head turns decreases. In the second case, the contour is concentrated around the nose and mouth. It requires much less material.

The next stage of research is to determine the area of contact of the obturation strip with the face. To do this, with the help of the *MatLab* ICP (iterative closest point) method, the "cloud" of half-mask points and the face are compared, with the coordinates that coincide indicated [24]. After this, the obtained results are analyzed in *Solidworks* program, the surface is constructed (Fig. 7), and its area is determined. The results of the obturator area calculations are shown in Table 4.

The protective properties of half masks can be preliminarily verified by theoretical calculation of the protection factor. To do this, let us determine the suction of air through gaps between the obturator (draught strip) and the face with a uniform distribution of surface stress across the width of the obturator area by the formula [25]:

$$Q_l = C_g \times C_u,$$

where $C_g = \frac{k_{\max}\Delta p}{l\mu}$; $k_{\max}$ is maximum diameter of the gap on the draught strip, m; Δp is pressure gradient, Pa; l is draught width, m; μ is dynamic viscosity of air, Pa s; C_u is coefficient of penetration through gaps [26].

$$C_u = \frac{k_g}{8\,(1 - k_g)},$$

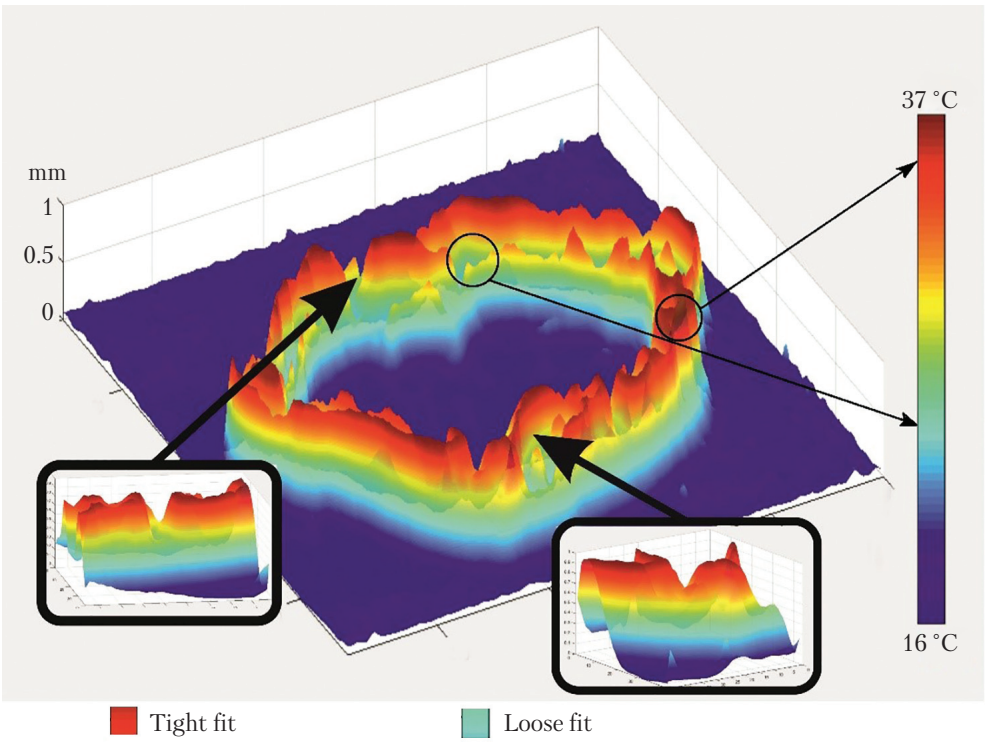

Fig. 8. Infrared image of obturator in the MathLab based on thermal imaging method

where k_g is coefficient of effectiveness of the use of surface of half mask obturator; ζ is coefficient of local losses.

E.S. Reiner recommends determination of the coefficient of local losses through gaps by the formula [25]:

$$\zeta = 2.5 + 5.5 \times 10^{-4}\left(\frac{l}{k_{\max}}\right).$$

The coefficient of the effectiveness of the use of surface of half mask obturator from the formula:

$$k_g = \frac{F_e}{F_o},$$

where F_e is working or effective surface of the obturator that fits well to the face, m^2; F_0 is the total area of half mask obturator, m^2.

The effective surface of half-mask obturator and the height of irregularities on the draught strip can be determined by thermographing its inner side that is worn on the face. The data have been processed in the *MathLab* program (Fig. 8).

The algorithm for converting thermal energy into images assumes that the coldest object from which the receiver obtains the least energy corresponds to black (the wavelength is 8 microns); the hottest object corresponds to light red color (wavelength is 12 microns). The entire dynamic range from the coldest to the hottest objects is divided into 256 gradations, each is evenly assigned with its shade. The lower the energy of the radiation, the closer the shade to black, and vice versa, the higher the energy, the closer the color to light red.

The thermogram of the surface of the obturation strip allows detecting the places of loose fit by the intensity of thermal radiation of the obturator surface in the infrared range and displaying the thermal field on the thermal imager display in the form of a color image. In other words, the location of the local temperature anomaly on the surface of the obturation strip is determined by varying color of the thermogram. The protection factors of respirators are given in Table 5.

The half masks designed based on dimensions of face length and width have the area of the obturator 1.4 times larger than the half masks modeled based on the face length and lip length. The research has allowed systematizing the existing approaches to the design of half masks and creating an algorithm for the development of PPERO (Fig. 9).

As a result, the algorithm for the design and manufacture of filter half masks has been developed and improved. It consists of several stages. At the first stage, it is necessary to determine the dimensions of potential consumer face, to input them into the 3D model of the head on which the obturator contour of a half mask is designed. The result is the shape of a half-mask model in which it is necessary to calculate the area of contact with the face. Of course, there are difficulties in

Table 4. **Area of Half Mask Fit to Face**

Option	The area of the obturator according to the areas of the face, cm^2				Total contact area, cm^2	Average thickness of obturator, cm
	Nose bridge	Right cheek	Left cheek	Chin		
1	4.2	21.3	20.9	10.8	57.2	0.9
2	3.2	13.4	12.8	9.3	38.7	0.6

Table 5. **Protective Effectiveness of Half Masks**

Option	Parameters						
	Pressure gradien t, Δp, Pa	Total loss of air, Q_0, m/s	Maximum height of irregularities , k_{max}, mm	Effectiveness factor, k_g	C_g, m^3/s	Coefficient of penetration, C_u	Protection factor $K_з = Q_0/Q_1$
1	75	0.0015	0.04	0.8	5.2×10^{-5}	1.25	28.7
2			0.06	0.7	8.4×10^{-5}	0.74	17.9

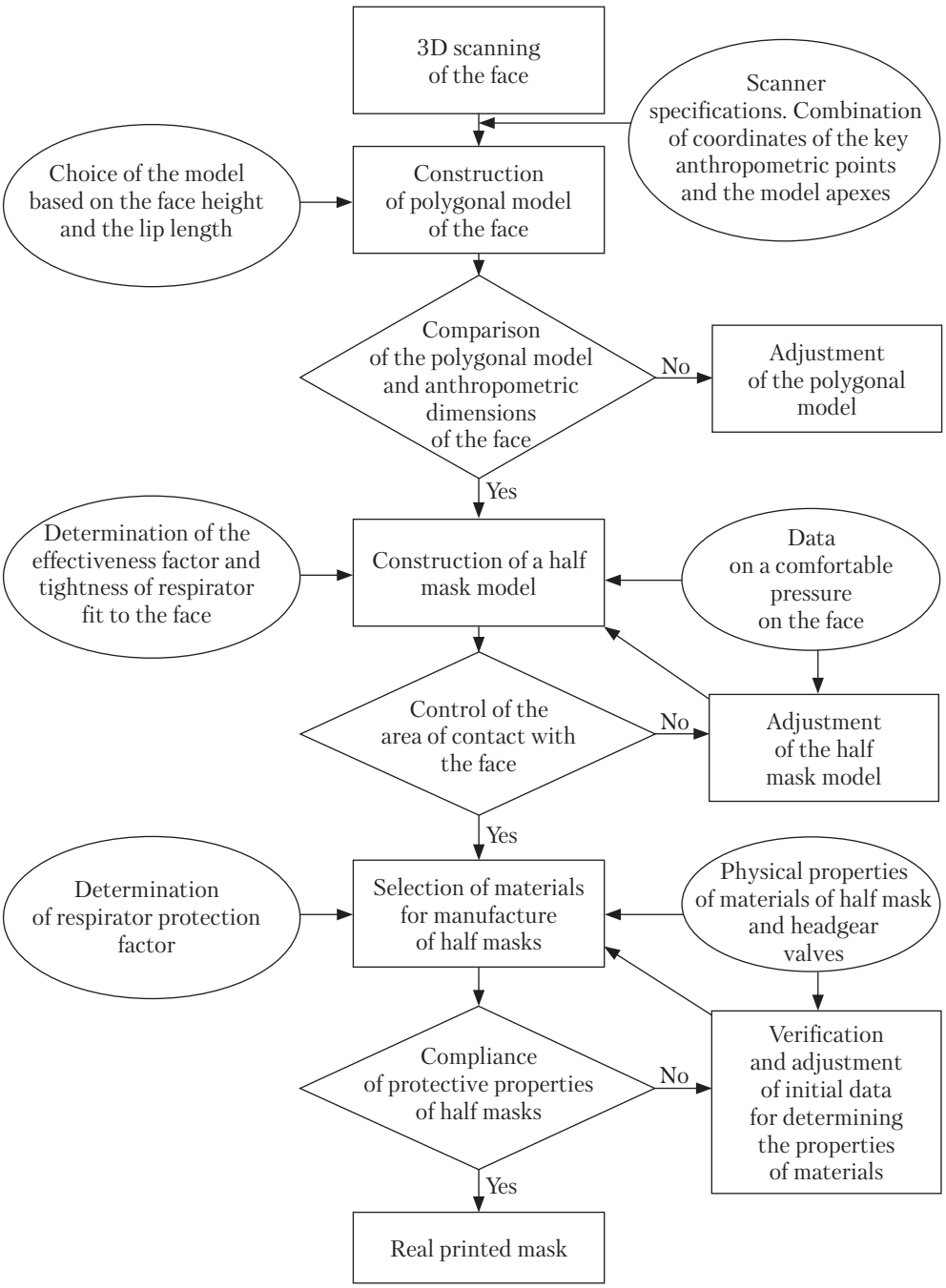

Fig. 9. Filter half mask design flowchart

calculations, which are associated with different thickness and elasticity of the face. However, their influence on the obturator design is minimized by conducting field studies of the experimental sample. Further, the appropriate filter structure (number of layers. the need for an exhalation valve) and the type of filter material will be selected proceeding from the concentration and

properties of the predicted inhaled aerosols and operating conditions. This process has been described in detail in many publications [4, 27]. It should be noted that the modern range of filter materials allows ensuring a high degree of air purification.

The above calculations have enabled estimating the insulation coefficient of half masks. It is logical that as the area of the obturation strip increases, the probability of additional channels for penetration of aerosol particles into the undermask space decreases. It is assumed [28] that to ensure a sufficient tightness, it is necessary to make an obturator that can repeat the face contours of soft elastomeric materials, separately from the half mask. There are similar developments of half masks from well-known manufacturers (for example, the Advantage 200 respirator). However, this assumption needs further verification.

It should be noted that the further research is necessary to develop the design of obturator for different types of faces and to implement field studies of half masks designed in this way.

Hence, in the course of the research, the main anthropometric parameters of human face, which most influence the design of half masks have been identified. Later, a polygonal 3D model of the human head has been built based on them. Proceeding from the established basic coordinates of the human head, the surface of the half-mask has been determined by the interpolation method, and the area of the half mask contact with the face has been calculated by the ICP method. The area of the obturation strip and its perimeter, as well as the insulation coefficient of half masks have been calculated. It has been shown that in half masks built on the main dimensions of the face length and width, the area of the obturator is 2.5 times larger than in half masks designed based on the length of the face and the lips. The research has allowed systematizing the available approaches to design of half masks and developing algorithm of design of PPERO. An algorithm for 3D-design of half masks has been developed. It differs from others by the fact that at each stage of converting the scanned image of worker's face into a digital image of the half mask surface that can be made on a 3D printer, the image conformity and the tightness of the prototype fit to the face are verified, and the protection factor is preliminarily calculated. A method for checking the quality of respirators based on determining the area of the half mask and the clamping force of the half mask to the face has been developed. It enables establishing the protection factor of respirators at the design stage and helps reduce errors while shaping the mask frame.

REFERENCES

1. Strilets, V. M., Vasyliev, M. V. (2010). Analysis of protective properties individual protective devices designed for working under conditions of toxic release. *Scientific Works of Kharkiv National Air Force University*, 1(23), 197—200 [in Ukrainian].
2. Kirillov, V. F., Buchnev, A. A., Chirkin, A. V. (2013). On individual respiratory organs protective devices of workers. *FSBSI "RI of Occupational Health"*, 4, 25—31. doi: 10.17686/sced_rusnauka_2013—1033 [in Ukrainian].
3. Kovacs, L., Immermann, A., Brockmann, G. (2006). Three-dimensional recording of the human face with a 3D laser scanner. *J. Plast. Reconstr. Aesthet. Surg.*, 59(11), 1193—1202.
4. Ennan, A. A., Belinskii, Ye. Ye., Klimova, L. V., Baidenko, V. I. (2001, September). Mathematical modeling of constructions of a lightened respirator of 'Snezhok' type. *Works of the 1st International research and practical conference "Environmental protection, health, safety in welding engineering" (15 Sept. 2001, Odessa)*. Odessa [in Ukrainian].
5. Tretiakova, L. D., Podobed, I. M., Zubkov, A. A. (2014). New individual protective devices for performing emergency-rescue works. *Information bulletin on labor occupational safety*, 1(72), 98—103 [in Ukrainian].
6. Kovaliov, P. A., Strilets, V. M., Yelizarov, O. V., Bezuhlov, O. Ye. (2005). *Basics of developing and applying devices on pressurized air*. Kharkiv: ATsZU [in Ukrainian].
7. Andrusiak, Z. V., Bolibrukh, B. V., Loik, V. B., Krasutskaya, I. M. (2015). An issue of developing effective individual protective devices of rescuers in an emergency at hazardous chemical sites. *Zeszyty Naukowe SGSP*, 56(4), 111—134.

8. Ostapenko, N. V., Lutsker, T. V., Rubanka, A. I., Kolisnichenko, O. V. (2016). Generalized systematization of special-purpose products. *Theory and practice of design*, 10, C. 122—143 [in Ukrainian].
9. Kolosnychenko, M. V., Zubkova, L. I., Pashkevych, K. L., Polka, T. O., Ostapenko, N. V., Vasilieva, I. V., Kolosnichenko, O. V. (2014). *Ergonomics and design. Designing modern clothing: learning guide*. Kyiv [in Ukrainian].
10. Cheberiachko, S. I., Radchuk, D. I., Cheberiachko, Yu. I., Frundin, V. Yu. (2016). Experimantal research on influence of air humidity on protective properties of electrete filters. *Mining electromechanics and automation*, 1(96), 59—66 [in Ukrainian].
11. Vasyliev, M. V., Strilets, V. M., Kovrehin, V. V. (2010). Analysis of tightness of a complex of individual protective devices of the first type. *Problems of emergences*, 11, 29—38 [in Ukrainian].
12. Anderson, N. J., Cassidy, P. E., Janssen, L. L., Dengel, D. R. (2006). Peak Inspiratory Flows of Adults Exercising at Light, Moderate and Heavy Work Loads. *Journal of the International Society for Respiratory Protection*, 23, 53—61.
13. Eshbaugh, J. P., Gardner, P. D., Richardson, A. W. (2009). №95 and P100 respirator filter efficiency under high constant and cyclic flow. *Journal Occup. Environ. Hyg.*, 6(1), 52—61.
14. Haruta, H., Honda, T., Eninger, R. (2009). Experimental and theoretical investigation of the performance of №95 respirator filters against ultrafine aerosol particles tested at constant and cyclic flows. *Journal Int. Soc. Respir. Prot.*, 25, 75—88.
15. Potapenko, I. A. (2010). Hydrodynamic resistance of a filtering element of a dust respirator. *Mine-rescue work: Collected Scientific Works*, 47, 133—141 [in Ukrainian].
16. Cheberiachko, S. I., Radchuk, D. I., Cheberiachko, Yu. I. (2016). Methods for selecting testers for studying filtering respirators. *Metrology and devices*, 2, 36—40 [in Ukrainian].
17. Oestenstad, R. K., Dillion, H. K., Perkins, L. L. (1990). Distribution of faceseal leak sites on a half-mask respirator and their association with facial dimensions. *American Industrial Hygiene Association Journal*, 5(51), 285—290. doi: 10.1080/15298669091369664.
18. Oestenstad, R. K., Perkins, L. L. (1992). An assessment of critical anthropometric dimensions for predicting the fit of a halfmask respirator. *American Industrial Hygiene Association Journal*, 53(6), 639—644.
19. Oestenstad, R. K., Elliot, L. J., Beasley, T. M. (2007). The effect of gender and respirator brand on the association of respirator fit with facial dimensions. *Journal of Occupational and Environmental Hygiene*, 4(12), 923—930.
20. Brazile, W. J., Buchan, R. M., Sandfort, D. R., Melvin, W., Johnson, J. A., Charney, M. (1998). Respirator fit and facial dimensions of two minority groups. *Journal of Occupational and Environmental Hygiene*, 13, 233—237. doi: 10.1080/1047322X.1998.10390073.
21. Han, D. H., Choi, K. L. (2003). Facial dimensions and predictors of fit for half-mask respirators in Koreans. *AIHA J.*, 64(6), 815—822. doi: 10.1202/501.1.
22. Zhuang, Z., Bradtmiller, B., Shaffer, R. E. (2007). New respirator fit test panels representing the current U.S. civilian work force. *Journal of Occupational and Environmental Hygiene*, 4(9), 647—659. doi: 10.1080/15459620701497538.
23. Alma Maria Jennifer A. Gutierrez, Melissa D. Galang, Rosemary R. Seva, Michelle C. Lu, Diana Rose S. (2014). Designing an improved respirator for automotive painters. *International Journal of Industrial Ergonomics*, 44(1), 131—139.
24. Blanz, V., Vetter, T. (1999). A morphable model for the synthesis of 3D faces. *In:* 26th Annual Conference *on* Computer Graphics *and* Interactive Techniques*, ACM Press, Los Angeles*, 187—194.
25. Ashkenazy, A. V. (2003). *Basic theory and computational algorithms*. Tver: Pub. house of the Tver State University.
26. Ogar, P. M., Gerasimov, S. V., Sukhov, O. Yu., Glinov, S. N. (2001). Modelling of mass-transfer through the jointing of rough surface. *Mathematic modelling, numerical methods and programme systems: Interuniversity thematic collection of works/SPbGASU*, 7, 108—116 [in Russian].
27. Ogar, P. M., Tarasov, V. A., Daineko, A. A. (2010). On certain common regularities of elastoplastic implementation of a spherical indenter. *Systems. Methods. Technologies*, 4(8), 38—43 [in Russian].
28. Zhuang, Z., Coffey, C. C., Jensen, P. A., Campbell, D. L., Lawrence, R. B., Myers W. R. (2004). Correlation Between Quantitative Fit Factors and Workplace Protection Factors Measured in Actual Workplace Environments at a Steel Foundry. *American Industrial Hygiene Association Journal*, 64 (6), 730—739. doi: 10.1202/475.1.

Received 25.04.19
Revised 27.05.19
Accepted 10.06.19

С.І. Чеберячко, Ю.І. Чеберячко, І.А. Шайхлісламова
Національний технічний університет «Дніпровська політехніка»,
просп. Д. Яворницького, 19, Дніпро, 49005, Україна,
+380 56 744 1411, +380 56 247 0810, rector@nmu.org.ua

ПРОЄКТУВАННЯ ПІВМАСОК ФІЛЬТРУВАЛЬНИХ РЕСПІРАТОРІВ

Вступ. Серед професійних захворювань хвороби органів дихання є найрозповсюдженішими в світі, основною причиною виникнення яких є забруднення робочої зони шкідливими аерозолями та використання невідповідних антропометричним розмірам обличчя засобів індивідуального захисту органів дихання.

Проблематика. Ефективність фільтрувальних респіраторів залежить від двох компонентів: часу захисної дії фільтрів та ізольованих властивостей півмасок. Це вимагає проведення відповідних досліджень для побудови конструкцій півмасок, які дозволять забезпечити високі ізоляційні властивості.

Мета. Підвищення захисної дії фільтрувальних респіраторів шляхом удосконалення їхньої конструкції, яка відповідає антропометричним параметрам обличь.

Матеріали й методи. Для побудови поверхні півмаски застосовано рівняння вільної енергії вигнутої довільної пластинки, яке описується двовимірною сплайн-поверхнею, а її невідомі коефіцієнти встановлюють методом лінійної інтерполяції на основі даних тривимірних координат ключових точок антропометричних рис обличчя.

Результати. Визначено закономірності формування поверхні півмаски, ґрунтуючись на даних тривимірних координат ключових точок антропометричних параметрів обличчя. Розроблено метод вимірювання температури поверхні обтюратора тепловізором на основі опрацювання вихідних сигналів, що дозволяє здійснювати оперативний контроль місць утворення зазорів уздовж смуги обтюрації, виявляти погіршення ізолювальних властивостей протипилового респіратора та обчислювати коефіцієнт його захисту.

Висновки. Розроблено алгоритм проєктування півмасок з урахуванням результатів 3D-сканування обличь, створення цифрових моделей голови та на їхній основі — поверхні півмасок і конструкції обтюратора. Визначено раціональні параметри фільтрувальної коробки, розміру вихідного отвору для забезпечення мінімального перепаду тиску та рівномірного розподілу пилового осаду на фільтрувальній поверхні.

Ключові слова: модель, півмаска, респіратор, обтюратор, коефіцієнт ізолювання.